www.lajss.org
Latin American Journal of Solids and Structures 4 (2007) 19–38

Optimization of passive constrained layer damping treatments applied to composite beams

Marcelo A. Trindade*

Department of Mechanical Engineering, São Carlos School of Engineering,
University of São Paulo, SP – Brazil

Abstract

The geometrical optimization of passive damping treatments applied to laminated composite beams is presented, using a sandwich/multilayer beam finite element model. The frequency dependence of the viscoelastic material properties is modeled using Anelastic Displacement Fields model. A complex-based modal reduction, followed by an equivalent real representation, is considered. Passive damping treatments consisting of viscoelastic layers sandwiched between two composite layers are studied, with the upper layer serving as a constraining layer (CL) and the lower one as a spacer (or stand-off) layer (SL). CL and SL plies number, thickness and orientation are considered as design parameters and are optimized using a genetic algorithm with eigenfrequency changes and weight constraints. A strategy for multicriteria optimization is presented using, as performance indices, the integral of transverse velocities and the damping factors of the first five eigenmodes and, as penalty functions, the total mass and the variation of eigenfrequencies due to the treatment. The results show that the use of a global cost function allows to improve the damping of structural vibrations while minimizing structure modification due to the treatment.

Keywords: vibration control, constrained layer damping, viscoelastic materials, optimization, genetic algorithms

1 Introduction

Sandwich structures with embedded viscoelastic materials are widely used in aerospace, aeronautical, automobile industries due to their benefic performance in attenuating structural vibrations [20]. The vibratory energy is dissipated through the shear strains induced in the soft viscoelastic layer by the relative displacements of the stiffer surface layers. The mechanical modeling of a three-layer metal-viscoelastic-metal beam was first developed by Kerwin [10] towards the end of the fifties. He considered simply supported sandwich beams supposing only transverse shear for the core and negligible bending rigidity for the core and the constraining layer. DiTaranto [4] and Mead and Markus [18] extended the work of Kerwin to treat arbitrary

*Corresp. author email: trindade@sc.usp.br Received 8 June 2006; In revised form 14 November 2006

Nomenclature

$\mathbf{A}$	State space dynamics matrix.
$\mathbf{C}$	State space output matrix.
$\mathbf{D}$	Damping matrix.
$\bar{\mathbf{D}}$	ADF augmented damping matrix.
Δ_i	Viscoelastic material ADF parameter.
$\mathbf{F}_m$	Mechanical forces vector.
$\bar{\mathbf{F}}_m$	ADF augmented mechanical forces vector.
$G^*(\omega)$	Complex shear modulus of the viscoelastic core.
G_0	Static shear modulus of the viscoelastic core.
h_v	Viscoelastic layer thickness.
h_T	Constraining layer laminaes thickness.
h_B	Spacer layer laminaes thickness.
H_T	Constraining layer total thickness.
H_B	Spacer layer total thickness.
J_1	Squared-velocities integral performance index.
J_2	Squared-damping factors performance index.
J_3	Damping treatment mass penalty function.
J_4	Squared-eigenfrequency variations penalty function.
J_g	Global cost function.
$\bar{\mathbf{K}}$	ADF augmented stiffness matrix.
$\mathbf{K}_c$	Core stiffness matrix.
$\mathbf{K}_f$	Faces stiffness matrix.
$\mathbf{M}$	Mass matrix.
$\bar{\mathbf{M}}$	ADF augmented mass matrix.
n_T	Number of laminaes of constraining layer.
n_B	Number of laminaes of spacer layer.
$\eta(\omega)$	Viscoelastic loss factor.
Ω_i	Viscoelastic material ADF parameter.
$\mathbf{p}$	Vector of state space perturbations.
ϕ_T	Orientation angle of the first ply of constraining layer.
ϕ_B	Orientation angle of the first ply of spacer layer.
$\mathbf{q}$	Degrees of freedom vector.
$\mathbf{x}$	Vector of state variables.
$\hat{\mathbf{x}}$	Vector of reduced state variables.

boundary conditions and forced vibrations. From these and more recent studies [17], it is clear that the damping performance of such structures depends on geometrical and material properties of each layer. In some cases, passive damping performance may be limited by geometrical and weight constraints so that it must be improved by active means [11, 23, 27].

One additional difficulty for the design and analysis of passive constrained layer damping (PCLD) treatments is that viscoelastic materials properties are frequency- and temperature-dependent. Hence, modeling of the frequency dependence of stiffness and damping properties of viscoelastically damped structures has been studied by several research groups during the last two decades. Methods based on fractional derivatives [1, 5] and internal variables, such as Anelastic Displacements Fields (ADF) [12, 13] and Golla-Hughes-McTavish (GHM) [7, 16] were proposed to allow precise time- and frequency-domain analyses of structures with viscoelastic elements. Although more complex, these methods have proven to be superior to the traditional Modal Strain Energy (MSE) method used in most commercial softwares for finite element analysis. A previous study [25] has shown that, although ADF and GHM models yield similar results for both time and frequency responses of beams with viscoelastic constrained layer damping treatments, ADF should be preferred since it contains less parameters to be fitted and it leads to smaller system dimensions. The use of these and other methods for the identification of viscoelastic materials damping behavior also has received considerable attention in recent years [3,5]. The temperature dependence has received much less attention based on the assumption that temperature changes are slow compared to the structure's dynamics [24]. However, for applications with significant or fast temperature variations, proper modeling and analysis of this effect should be performed [2, 14, 21].

The performance of viscoelastic PCLD treatments can be maximized by proper choice of materials and geometry. This could be achieved by using some optimization methodology as in [8,15,19,28]. Hao and Rao [8] presented a procedure for the optimization of simply supported beams covered with a PCLD treatment with the objective of maximizing the damping while minimizing the mass within given temperature and frequency ranges. Marcelin *et al.* [15] performed an optimization study of PCLD treatments covering one and several portions of a beam. They considered treatment dimensions and locations as design variables and the damping factor as objective function. Zheng *et al.* [28] presented the optimization of the vibrational energy of beams with PCLD treatments considering treatment location and length and viscoelastic material shear modulus as design variables. They used a genetic algorithm (GA) based optimization methodology. GAs were already used by other authors [22] for design optimization. Their main advantage is that, unlike conventional optimization techniques, they do not require continuity or differentiability of the objective function with respect to design variables and the probability of finding a local optimum is smaller [6].

This work aims to present a study on the geometrical optimization of passive damping treatments applied to laminated composite beams. This is made using a finite element (FE) model proposed in [26], able to handle sandwich beams with laminated surface layers and viscoelastic core. The frequency dependence of the viscoelastic material properties is modeled using ADF

model [12, 13]. A complex-based modal reduction, proposed in [25], is used and an equivalent real representation of the reduced-order system is constructed. The damping treatments consist of viscoelastic layers sandwiched between two composite layers. The upper one serving as constraining layer (CL) and the lower one as spacer (or stand-off) layer (SL). In the present work, CL and SL plies number, thickness and orientation are considered as design parameters. The performance of the viscoelastic damping treatment is optimized using a GA proposed by Houck *et al.* [9] with eigenfrequency changes and weight constraints. A strategy for multicriteria optimization is presented using as performance indices the integral of transverse velocities, to be minimized, and the damping factors of the first five eigenmodes, to be maximized. In addition, the total mass of the treatment and the variation of the structure eigenfrequencies due to the treatment are used as penalty cost functions.

2 Sandwich/multilayer beam finite element model

In a previous work [26], a finite element model able to deal with sandwich beams with viscoelastic core and multilayer faces was presented. The laminated faces are supposed to behave as Bernoulli-Euler beams while Timoshenko hypothesis are retained for the core, to allow shear strains to occur in the viscoelastic material layer. The axial (x direction) and transverse (z direction) displacements of the top, bottom and core layers are written in terms of four main variables: mean $\bar{u}(x)$ and relative $\tilde{u}(x)$ axial displacements of the top and bottom layers midplanes, constant through-thickness transverse displacement $w(x)$, and bending rotation $\partial w(x)/\partial x$. Lagrange linear shape functions are considered for the mean and relative axial displacements while Hermite cubic ones are considered for the transverse displacement. A schematic diagram of the finite element considered is shown in Figure 1.

Full three-dimensional constitutive matrices are considered for each material. These are then tensor-transformed according to the corresponding layer orientation in the xy plane. The transformed three-dimensional constitutive matrices are finally reduced using the xy plane-stress assumption (see appendix). Consequently, composite material orientation is properly accounted for in the FE model.

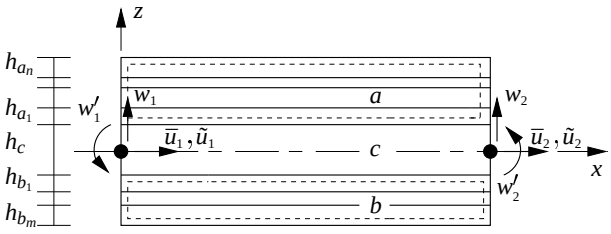

Figure 1: Schematic representation of the sandwich/multilayer beam finite element.

Considering constant material properties, the assembled equations of motion may be written

in the form [26]

$$\mathbf{M}\ddot{\mathbf{q}} + \mathbf{D}\dot{\mathbf{q}} + (\mathbf{K}_f + \mathbf{K}_c)\,\mathbf{q} = \mathbf{F}_m \tag{1}$$

where $\mathbf{q}$ is the dofs vector, composed by the nodal mean and relative axial displacements, deflections and bending rotations. $\dot{\mathbf{q}}$ and $\ddot{\mathbf{q}}$ are respectively the velocity and acceleration vectors. $\mathbf{M}$, $\mathbf{K}_f$ and $\mathbf{K}_c$ are the mass and stiffness matrices, of the layered faces and core, obtained by the FE model. $\mathbf{D}$ is a viscous damping matrix introduced a posteriori and $\mathbf{F}_m$ is a mechanical load used as perturbation input.

It is known that the viscoelastic material properties depend on the excitation frequency and operating temperature. In the present work, only frequency dependence of the viscoelastic material is considered using ADF model [12, 13]. Hence, the operating temperature is assumed constant and the self-heating of the viscoelastic material is neglected.

Supposing a frequency-independent Poisson's ratio, one may assume $\mathbf{K}_c = G^*(\omega)\bar{\mathbf{K}}_c$. Hence, for a given frequency, the discretized equations of motion (1) may be rewritten as

$$\{-\omega^2\mathbf{M} + \mathrm{j}\omega\mathbf{D} + [\mathbf{K}_f + G^*(\omega)\bar{\mathbf{K}}_c]\}\tilde{\mathbf{q}} = \tilde{\mathbf{F}}_m \tag{2}$$

where $G^*(\omega)$ is the complex frequency-dependent shear modulus of the viscoelastic layer, represented in the ADF model as a series of functions in the frequency-domain

$$G^*(\omega) = G_0 + G_0 \sum_i \Delta_i \frac{\omega^2 + \mathrm{j}\omega\ \Omega_i}{\omega^2 + \Omega_i^2} \tag{3}$$

and j states for $\mathrm{j} = \sqrt{-1}$. The material parameters G_0, Δ_i and Ω_i must be curve-fitted relative to the measurements of $G^*(\omega)$. Notice that, from Eq. (3), the relaxed or static modulus is clearly $G_0 = G^*(0)$. In the present work, a nonlinear least squares optimization method was used to evaluate the ADF parameters. Figure 2 shows the measured and approximated storage modulus (G') and loss factor (η) for 3M ISD112 viscoelastic material at 27°C, where

$$G^*(\omega) = G'(\omega) + \mathrm{j}G''(\omega) = G'(\omega)[1 + \mathrm{j}\eta(\omega)] \tag{4}$$

As shown in Figure 2, both storage modulus and loss factor are well represented by three series of ADF parameters. Nevertheless, these material parameters are valid only in the frequency-range considered, that is the frequency-range where material properties were measured or furnished by the manufacturer. Therefore, it is necessary to ensure a reasonable behavior of ADF-represented material properties outside the frequency-range, since arbitrary external perturbations will generally excite modes lying on this interval. Required asymptotical properties are

$$\begin{cases} \lim\limits_{\omega\to 0} G^*(\omega) = G_0 \\ \lim\limits_{\omega\to\infty} G^*(\omega) = G_\infty \end{cases}, \quad \text{where } G_\infty > G_0 \in \mathbb{R}^+ \tag{5}$$

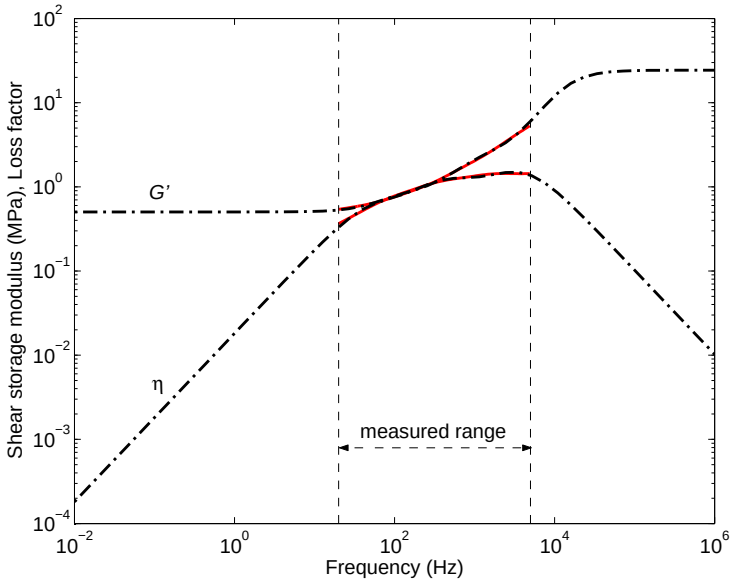

Figure 2: Frequency-dependence of 3M ISD112 viscoelastic material properties at 27°c (solid line) and curve-fit using three series of ADF parameters (dashed line).

meaning that the shear modulus tends to its static (relaxed) and instantaneous (unrelaxed) values at the boundaries 0 and ∞, respectively. This also imposes that $\eta(0) = \eta(\infty) = 0$, that is, dissipation only occurs in the transition region. One may notice from Figure 2 that these properties are satisfied by the parameters considered. Hence, the three series of ADF parameters presented in the appendix are used for the numerical analyses presented in this work.

The ADF model allows to eliminate the frequency-dependence of the stiffness matrix of Eq. (2) while still accounting for the viscoelastic behavior. This is done through the inclusion of n series of ADF dissipative dofs $\mathbf{q}_i^d$ $(i = 1, \ldots, n)$, such that the global dofs vector $\mathbf{q} = \mathbf{q}^e + \sum_i \mathbf{q}_i^d$ (elastic + dissipative) is replaced by the elastic part only $\mathbf{q}_e$ in the viscoelastic stiffness term. Then, replacing Eq. (3) in Eq. (2), leads to the following time-domain augmented system [25]

$$\bar{\mathbf{M}}\ddot{\bar{\mathbf{q}}} + \bar{\mathbf{D}}\dot{\bar{\mathbf{q}}} + \bar{\mathbf{K}}\bar{\mathbf{q}} = \bar{\mathbf{F}}_m \tag{6}$$

with

$$\bar{\mathbf{M}} = \begin{bmatrix} \mathbf{M} & \mathbf{0} \\ \mathbf{0} & \mathbf{0} \end{bmatrix} \; ; \; \bar{\mathbf{D}} = \begin{bmatrix} \mathbf{D} & \mathbf{0} \\ \mathbf{0} & \mathbf{D}_{dd} \end{bmatrix} \; ; \; \bar{\mathbf{F}}_m = \begin{bmatrix} \mathbf{F}_m \\ \mathbf{0} \end{bmatrix}$$

$$\bar{\mathbf{K}} = \begin{bmatrix} \mathbf{K}_f + \mathbf{K}_c^\infty & \mathbf{K}_{qd} \\ \mathbf{K}_{qd}^T & \mathbf{K}_{dd} \end{bmatrix} \; ; \; \bar{\mathbf{q}} = \mathrm{col}\left(\mathbf{q},\ \mathbf{q}_1^d,\ \ldots,\ \mathbf{q}_n^d\right)$$

where

$$\mathbf{D}_{dd} = G_\infty \,\mathrm{diag}\left(\tfrac{C_1}{\Omega_1}\Lambda \;\cdots\; \tfrac{C_n}{\Omega_n}\Lambda\right) \;;$$

$$\mathbf{K}_{dd} = G_\infty \,\mathrm{diag}\left(C_1\Lambda \;\cdots\; C_n\Lambda\right) \;;\; \mathbf{K}_{qd} = [-\mathbf{K}_c^\infty\mathbf{T} \;\cdots\; -\mathbf{K}_c^\infty\mathbf{T}]$$

and $\mathbf{K}_c^\infty = G_\infty\bar{\mathbf{K}}_c$, $G_\infty = G_0(1+\sum_i \Delta_i)$, $C_i = (1+\sum_i \Delta_i)/\Delta_i$. Λ is a diagonal matrix of non vanishing eigenvalues of $\mathbf{K}_c^\infty$ and $\mathbf{T}$ is the corresponding eigenvectors matrix.

3 State space model construction

In order to eliminate the apparent singularity of the system in Eq. (6) and to provide a transformation to an "elastic only" modal reduced model, Eq. (6) is then rewritten in a state space form. Therefore, a state vector $\mathbf{x}$ is formed by the augmented vector $\bar{\mathbf{q}}$ and the time-derivative of the mechanical dofs vector $\dot{\mathbf{q}}$. The time-derivatives of the dissipative dofs $\mathbf{q}_i^d$ may not be considered since these variables are massless. This leads to

$$\begin{aligned} \dot{\mathbf{x}} &= \mathbf{A}\mathbf{x} + \mathbf{p} \\ \mathbf{y} &= \mathbf{C}\mathbf{x} \end{aligned} \tag{7}$$

where the perturbation vector $\mathbf{p}$ is the state distribution of the mechanical loads $\mathbf{F}_m$ and the output vector $\mathbf{y}$ is, generally, composed of the measured quantities, written in terms of the state vector $\mathbf{x}$ through the output matrix $\mathbf{C}$. The system dynamics are determined by the square matrix $\mathbf{A}$. Matrices and vectors of the system in Eq. (7) are

$$\mathbf{A} = \begin{bmatrix} \mathbf{0} & \mathbf{0} & \cdots & \mathbf{0} & \mathbf{I} \\ \frac{\Omega_1}{C_1}\mathbf{T}^T & -\Omega_1\mathbf{I} & & \mathbf{0} & \mathbf{0} \\ \vdots & & \ddots & & \mathbf{0} \\ \frac{\Omega_n}{C_n}\mathbf{T}^T & \mathbf{0} & & -\Omega_n\mathbf{I} & \mathbf{0} \\ -\mathbf{M}^{-1}(\mathbf{K}_f+\mathbf{K}_c^\infty) & \mathbf{M}^{-1}\mathbf{K}_c^\infty\mathbf{T} & \cdots & \mathbf{M}^{-1}\mathbf{K}_c^\infty\mathbf{T} & -\mathbf{M}^{-1}\mathbf{D} \end{bmatrix} \tag{8}$$

$$\mathbf{x} = \begin{bmatrix} \bar{\mathbf{q}} \\ \dot{\mathbf{q}} \end{bmatrix} \;;\; \mathbf{p} = \begin{bmatrix} \mathbf{0} \\ \mathbf{M}^{-1}\mathbf{F}_m \end{bmatrix} \;;\; \mathbf{C} = \begin{bmatrix} \mathbf{C}_{\bar{q}} & \mathbf{C}_{\dot{q}} \end{bmatrix} \;;$$

where $\mathbf{C}_{\bar{q}}$ and $\mathbf{C}_{\dot{q}}$ are the output matrices relative to the augmented dofs vector $\bar{\mathbf{q}}$ and mechanical dofs derivatives $\dot{\mathbf{q}}$, respectively.

3.1 Complex modal reduction

The dimension of the state space system in Eq. (7) is generally too large for analysis and design. Thus, a complex-based modal reduction is applied to this system, neglecting the contributions

of the viscoelastic relaxation modes and the elastic modes related to eigenfrequencies out of the frequency-range considered. Hence, the eigenvalues matrix Λ and, left $\mathbf{T}_l$ and right $\mathbf{T}_r$, eigenvectors of $\mathbf{A}$ are first evaluated from

$$\mathbf{A}\mathbf{T}_r = \Lambda\mathbf{T}_r \;;\; \mathbf{A}^T\mathbf{T}_l = \Lambda\mathbf{T}_l \tag{9}$$

so that $\mathbf{T}_l^T\mathbf{T}_r = \mathbf{I}$, then decomposed as following

$$\Lambda = \begin{bmatrix} \Lambda_r & \mathbf{0} & \mathbf{0} \\ \mathbf{0} & \Lambda_n & \mathbf{0} \\ \mathbf{0} & \mathbf{0} & \Lambda_d \end{bmatrix} \;;\; \mathbf{T}_l = [\mathbf{T}_{lr}\ \mathbf{T}_{ln}\ \mathbf{T}_{ld}] \;;\; \mathbf{T}_r = [\mathbf{T}_{rr}\ \mathbf{T}_{rn}\ \mathbf{T}_{rd}] \tag{10}$$

where Λ_r is the retained elastic eigenvalues matrix and $\mathbf{T}_{lr}$ and $\mathbf{T}_{rr}$ are its left and right corresponding eigenvectors matrices, respectively. Λ_n and Λ_d correspond to the neglected elastic and relaxation eigenvalues, respectively. $\mathbf{T}_{ln}$, $\mathbf{T}_{rn}$, $\mathbf{T}_{ld}$ and $\mathbf{T}_{rd}$ are their corresponding left and right eigenvectors. Consequently, the state vector is approximated as $\mathbf{x} \approx \mathbf{T}_{rr}\mathbf{x}_r$ and, using Eqs. (9) and (10), the Eq. (7) may be reduced to

$$\begin{aligned} \dot{\mathbf{x}}_r &= \Lambda_r\mathbf{x}_r + \mathbf{T}_{lr}^T\mathbf{p} \\ \mathbf{y} &= \mathbf{C}\mathbf{T}_{rr}\mathbf{x}_r \end{aligned} \tag{11}$$

3.2 Real representation of the reduced model

The main disadvantage of the reduced state space system in Eq. (11) is that its matrices are complex. Fortunately, since all overdamped (relaxation) modes were neglected, all elements of the system in Eq. (11) are composed of complex conjugates, such that

$$\begin{aligned} \Lambda_r &= \mathrm{diag}(\ldots, \lambda_j, \bar{\lambda}_j, \ldots) \\ \mathbf{T}_{lr}^T\mathbf{p} = \mathrm{col}(\ldots, \varphi_j, \bar{\varphi}_j, \ldots) \;;\; \mathbf{C}\mathbf{T}_{rr} &= \begin{bmatrix} \cdots & \phi_j & \bar{\phi}_j & \cdots \end{bmatrix} \end{aligned} \tag{12}$$

where λ_j $(j = 1, \ldots, r)$ are the retained elastic eigenvalues and $\bar{\lambda}_j$ their complex conjugates. To construct a real representation of the state space system in Eq. (11), one may use a state transformation $\hat{\mathbf{x}} = \mathbf{T}_c\mathbf{x}_r$, where $\mathbf{T}_c$ is defined as [27]

$$\mathbf{T}_c = \begin{bmatrix} \ddots & & & \\ & -\mathrm{j}\frac{1}{2\mathrm{Im}(\lambda_j)} & \mathrm{j}\frac{1}{2\mathrm{Im}(\lambda_j)} & \\ & & & \ddots \\ \ddots & & & \\ & \frac{1}{2} - \mathrm{j}\frac{1}{2}\frac{\mathrm{Re}(\lambda_j)}{\mathrm{Im}(\lambda_j)} & \frac{1}{2} + \mathrm{j}\frac{1}{2}\frac{\mathrm{Re}(\lambda_j)}{\mathrm{Im}(\lambda_j)} & \\ & & & \ddots \end{bmatrix} \tag{13}$$

so that the real state space system equivalent to Eq. (11) is

$$\begin{aligned} \dot{\hat{\mathbf{x}}} &= \hat{\mathbf{A}}\hat{\mathbf{x}} + \hat{\mathbf{p}} \\ \mathbf{y} &= \hat{\mathbf{C}}\hat{\mathbf{x}} \end{aligned} \tag{14}$$

where

$$\hat{\mathbf{A}} = \mathbf{T}_c \Lambda_r \mathbf{T}_c^{-1} = \begin{bmatrix} \mathbf{0} & & \mathbf{I} & \\ \ddots & & \ddots & \\ & -|\lambda_j|^2 & & 2\mathrm{Re}(\lambda_j) \\ & & \ddots & & \ddots \end{bmatrix}$$

$$\hat{\mathbf{p}} = \mathbf{T}_c \mathbf{T}_{lr}^T \mathbf{p} = \mathrm{col}(\ldots, \tfrac{\mathrm{Im}(\varphi_j)}{\mathrm{Im}(\lambda_j)}, \ldots, \mathrm{Re}(\varphi_j) + \mathrm{Im}(\varphi_j)\tfrac{\mathrm{Re}(\lambda_j)}{\mathrm{Im}(\lambda_j)}, \ldots)$$

$$\begin{aligned} \hat{\mathbf{C}} &= \mathbf{C}\mathbf{T}_{rr}\mathbf{T}_c^{-1} \\ &= \begin{bmatrix} \cdots & -2[\mathrm{Re}(\phi_j)\mathrm{Re}(\lambda_j) + \mathrm{Im}(\phi_j)\mathrm{Im}(\lambda_j)] & \cdots & 2\mathrm{Re}(\phi_j) & \cdots \end{bmatrix} \end{aligned}$$

It is clear that the eigenvalues of the real matrix $\hat{\mathbf{A}}$ are exactly the elements of Λ_r. In the form of Eq. (14), the new state variables $\hat{\mathbf{x}}$ represent the modal displacements and velocities.

4 Geometric optimization

To evaluate the geometric optimization of a PCLD treated beam, a host clamped-clamped composite beam, made of a AS4/3501-6 carbon-epoxy laminate (0/90/0/90/0) is considered, as shown in Figure 3. The beam length, width and thickness are $b = 25$ mm, $L = 1000$ mm and $h_b = 5$ mm. A passive damping treatment is proposed in order to minimize the structural vibration of the beam. The passive treatment considered here consists of a viscoelastic material layer sandwiched between two composite laminates, as presented in Figure 3. It has a length $a = 750$ mm and is located at $d = 125$ mm of the left end. Material properties are given in the appendix.

In this section, the state space system in Eq. (14), using the first ten bending modes, is considered to perform a geometric optimization of the passive damping treatment. As shown in Figure 3, h_v, H_T and H_B are the thicknesses of viscoelastic, constraining and spacer layers, respectively. The laminate constraining layer (CL) and spacer layer (SL) are made of, respectively, n_T and n_B cross-ply AS4/3501-6 carbon-epoxy laminaes of equal thicknesses (h_T and h_B). The angle of the first laminae is ϕ_T, for the CL, and ϕ_B, for the SL. These seven geometric properties of the damping treatment (h_v, h_T, h_B, n_T, n_B, ϕ_T, ϕ_B) are considered to be design parameters.

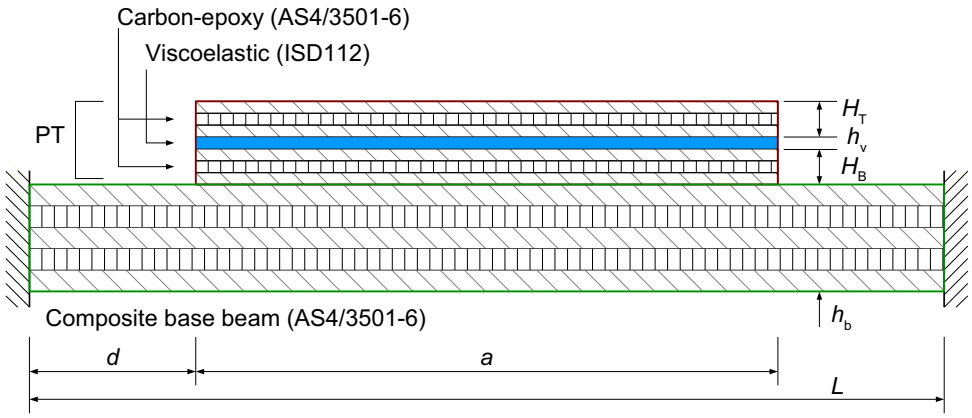

Figure 3: Composite base beam covered with a passive treatment (PT) made of a viscoelastic layer between two composite laminates.

4.1 GA optimization

A GA optimization is considered here. GAs are search algorithms based on "survival of the fittest" procedure among a structured set of parameters [6]. These algorithms, unlike conventional optimization techniques, do not require continuity or differentiability. Moreover, since they work with a population of points simultaneously, the probability of finding a local optimum is reduced. The GA optimization method starts from an initial population that evolves over a number of generations with the objective to produce better individuals. Basically, three operations are performed by the method: selection, reproduction and evaluation. In the selection phase, individuals of the population are compared using a payoff value, which is generally the performance index. Reproduction may be achieved either by combining two selected individuals or by mutation of some individuals. Notice that the population size does not change. The last operation evaluates the evolution of the entire population and decides for termination. Several techniques were developed for each GA operation. Details may be found in [6,9]. In the present work, a GA implementation for MATLAB, namely *Genetic Algorithm for Optimization Toolbox* (GAOT), developed by Houck, Joines and Kay [9], is used.

4.2 Performance index

Two objective functions were used. The first one is the sum of the integral of squared-velocities in seven equally-spaced points in the beam, that is,

$$J_1 = -\frac{1}{2}\int_0^T \dot{\mathbf{w}}^T \dot{\mathbf{w}} \mathrm{d}t \tag{15}$$

where $\dot{\mathbf{w}}$ is the vector of transverse velocities for the following selected points: $x/L = \{0.125, 0.250, 0.375, 0.500, 0.625, 0.750, 0.875\}$. This cost function furnishes a measure of the power

transmitted to the side opposite to the perturbation, which should be minimized. That is why, a negative value is used. An impulsive transverse force is applied at the midpoint of the beam ($x = L/2$) leading to a transient response of the transverse velocities, which are integrated in the interval $[0, T]$. T is the stabilization time of the structure output response.

The second objective function considered represents the sum of the squared damping factors of the first five bending natural modes, such that

$$J_2 = \frac{1}{2}\zeta^T\zeta \tag{16}$$

where ζ is a vector containing the selected damping ratios $\zeta = [\zeta_1, \zeta_2, \zeta_3, \zeta_4, \zeta_5]$. Only the first five bending modes were considered since it is assumed that higher frequency modes contributions to the pressure variation are much smaller.

In addition to these objective functions, due to practical reasons, two penalty functions are considered, namely the negative of the total mass of the damping treatment

$$J_3 = -m \quad = -ba\left[\rho_v h_v + \rho_c(H_T + H_B)\right] \tag{17}$$

where b is the width of the structure, and the sum of the squared variations in the first ten natural frequencies,

$$J_4 = -\frac{1}{2}(\omega_n - \omega_u)^T(\omega_n - \omega_u) \tag{18}$$

where ω_n and ω_u are the treated and untreated beam natural frequencies vector, respectively. These two penalty functions represent conditions often required in practical applications, since all modification in the properties of the structure must be minimized.

In addition to these objective and penalty cost functions, a global criterion method is considered in the present work. First, a global cost function is constructed using a linear combination of the cost functions presented above. It is defined as

$$J_c = \sum_i \alpha_i J_i \; ; \quad \alpha_i > 0 \tag{19}$$

Through proper choice of the weight factors α_i, the damping factors function may be maximized, while transverse velocities, treatment mass and eigenfrequencies variation may be minimized. The weight factors α_i should be chosen according to design and operation conditions. However, the global cost function J_c combines local cost functions with different dimensions and meanings, hence the choice of factors α_i is generally not easy. One possible solution to that is to perform the optimization using several combinations of weight factors according to the application needs and, then, choose the best suited combinations.

A second method to perform a multicriteria optimization consists in the minimization of each local cost function separately leading to a set of optimal performance indices J_1^*, J_2^*, J_3^* and J_4^*. Then, the global cost function to be minimized is written as

$$J_g = \sum_i \beta_i \left| \frac{J_i - J_i^*}{J_i^*} \right| \; ; \quad \beta_i > 0 \tag{20}$$

where weight factors β_i allow the prioritization of certain performance indices relative to the others. This global index provides a measure of the distance from the local performance indices for the global and local optimal solutions. This second method was preferred in the present work.

5 Results and discussion

Following the method presented in Eq. (20) for multicriteria optimization, first a GA optimization using local performance indices alone was performed. An initial population of 100 individuals is considered and evolution is performed along 50 generations. Selection is performed using normalized geometric ranking. Then, arithmetic crossover and non-uniform mutation operators are applied to produce new generations. Results are shown in Table 1. Minimization of the squared transverse velocities cost function J_1 leads to a very thick treatment ($h_{PT} = 7.95$ mm). This may be explained by the fact that a thick treatment increases the mass of the structure and, thus for a constant impulsive force, reduces the amplitude of transverse velocities. Although, this does not improve damping of structural vibrations, as observed by the small damping cost function ($J_2^* = 0.07$), the reduction of velocities amplitudes leads to small velocity integrals. The increase of thickness yields a large treatment mass and a significant variation of eigenfrequencies, as shown in Table 1 (J_3^* and J_4^* for $\min(J_1)$, respectively). It is clear that this treatment not only induce design complexities but also increases cost, since larger quantities of material are needed (2.53 mm of ISD112 viscoelastic material and (0/90/0) at 0.74 mm per laminae and (90/0/90/0) at 0.80 mm per laminae carbon-epoxy composite material).

The use of the cost function J_2, based on the first five bending modes damping factors, leads to a much thinner ($h_{PT} = 2.73$ mm) treatment. This also yields to a more than 60% lighter design as compared to the previous one. Nevertheless, the increase of mass, represented by the normalized cost function J_3^*, is still significant, as shown in Table 1. One may also notice that, although this optimization increases the damping factors and, thus reducing the stabilization time of the structural vibrations, it does yield to relatively large J_1^*. This is due to the fact that structural vibrations are quickly damped but output amplitudes are large compared to those of the previous design. The major problem of the damping maximization is the consequent variation of natural bending frequencies of the structure, as it can be observed by the largest value for J_4^* in Table 1 (second column).

The third cost function considered J_3, which is in fact a penalty function, is the total mass of the passive damping treatment. It is worthwhile to notice that the additional mass included in the structure may lead to serious problems since it may change the dynamic behavior of the structure. Hence, it should be minimized. As expected, its minimization leads to almost no

Table 1: Optimal geometric properties for the beam with passive damping treatment.

Parameter	$\min(J_1)$	$\min(J_2)$	$\min(J_3)$	$\min(J_4)$	$\min(J_g)$
J_1^*	1.00	2.11	4.57	4.02	2.80
J_2^*	0.07	1.00	0.25	0.20	0.99
J_3^*	39.13	14.54	1.00	2.56	12.09
J_4^*	3.63	5.37	2.68	1.00	8.39
h_v (mm)	2.53	0.09	0.07	0.03	0.18
h_T (mm)	0.74	0.53	0.02	0.39	0.42
ϕ_T (deg)	0	90	0	90	0
n_T	3	4	2	1	3
h_B (mm)	0.80	0.26	0.05	0.02	0.85
ϕ_B (deg)	90	0	90	0	90
n_B	4	2	2	4	1

treatment at all, as shown in Table 1. Only a very thin treatment ($h_{PT} = 0.21$ mm) is obtained. It should be noticed that the obvious minimum for the treatment mass is the absence of it, however in none of the cases studied in this work, the lower or upper bounds were attained. This may be explained by the fact that the GA distributes the initial population in a random form and only rarely will create new individuals near enough to the bounds, so that new generations could attain it.

The consequences of reducing treatment mass are that structural vibrations damping factors are diminished and the squared-velocity integral is the largest of all cases. However, it is clear that this design, as it will also be the case for the next one, is not an optimal one but, on the contrary, should be seen as a "counter-design" (or penalized design). Its importance relies on the fact that it will be used as reference to the global optimization problem. As it can also be observed in Table 1, this design leads to a significant variation in the natural frequencies of the structure (J_4^* for $\min(J_3)$), although almost no vibration damping is achieved.

The minimization of the second penalty function J_4 yields similar analysis as compared to the previous case, that is, the treatment thickness is only lower-bounded by the numerical precision of the GA used. One may notice, in Table 1, that, although incoherently, minimization of the variation of eigenfrequencies does not lead to minimization of treatment mass, and vice-versa, while both minimizations should lead to the absence of treatment.

The local optimal performance indices obtained are $J_1^* = -1.7180\ 10^4$, $J_2^* = 1.5662\ 10^{-2}$, $J_3^* = -4.8162\ 10^{-3}$ and $J_4^* = 6.7873\ 10^6$. These indices were used to minimize the global cost function defined in Eq. (20). It should be noticed that several solutions minimizing J_g may be found, hence generally the optimization must be performed several times until satisfactory results are obtained. The fifth column of Table 1 shows the optimal parameters and local performance indices for a chosen design. The optimal design is represented in Figure 4. One may notice that the normalized damping factor objective function is almost unitary. This is

because the following weight factors were considered: $\beta_1 = \beta_3 = \beta_4 = 1$ and $\beta_2 = 50$, in order to better improve the structural damping. Indeed, the first ten damping factors for the optimal design are $\{7.19, 7.59, 7.73, 8.32, 8.54, 8.56, 8.47, 8.10, 7.65, 6.96\}\%$.

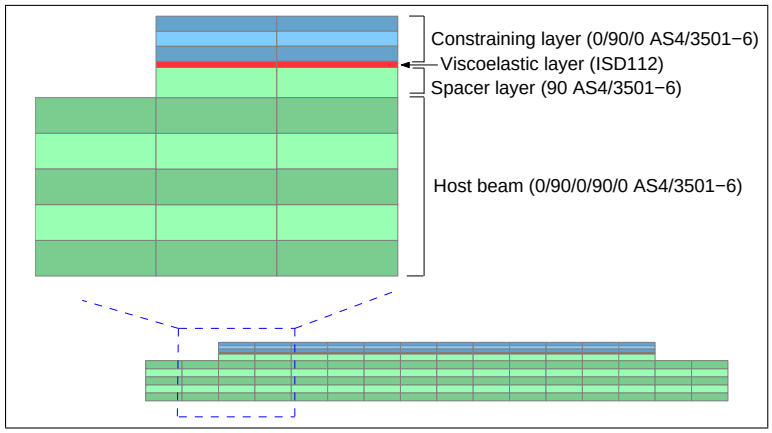

Figure 4: Optimal configuration $[\min(J_g)]$ of the passive damping treatment.

Next, the evolution process corresponding to the chosen design is analyzed in detail. The normalized global performance index (J_g) for the best and mean individuals of each generation is shown in Figure 5. It can be observed that both best and mean individuals converge to an almost optimality within less than 15 generations evolution. One may also notice, from Figure 5, that each "evolution" is first attained by the best individual and then, some generations after, by the mean individual.

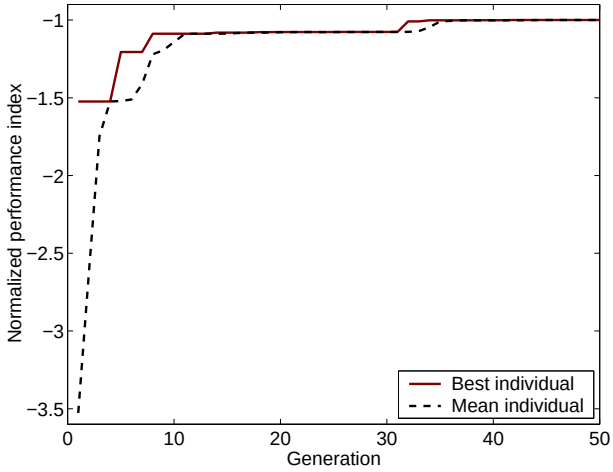

Figure 5: Normalized global performance index (J_g) for the best and mean individuals of each generation.

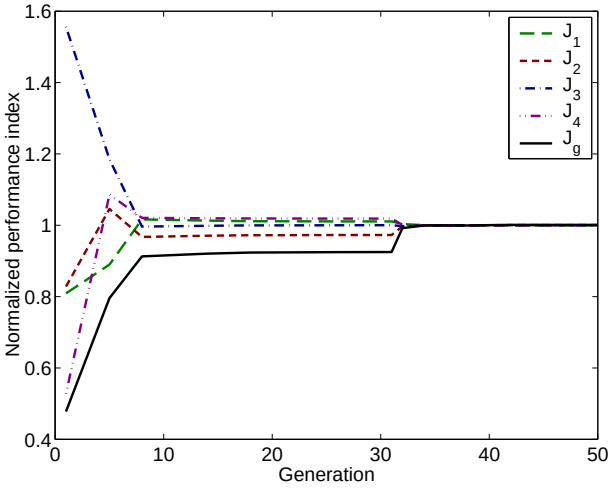

Figure 6: Normalized global and local performance indices for the best individuals of selected generations.

It is also worthwhile to analyze the behavior of the local performance indices along the population evolution. Figure 6 presents the normalized global J_g and local J_i ($i = 1, \ldots, 4$) performance indices for the best individuals of selected generations. Notice that while the global performance index converges monotonically to the optimal solution, local indices present some oscillation. Although the squared-velocities and eigenfrequencies variation indices, J_1 and J_4, should be minimized, one may see in Figure 6 that their minimum is for the initial population. These indices increase within generations. However, damping factors index J_2 is well maximized within the limitations of treatment mass. Indeed, as it may be observed in Figure 6, J_2 index is maximized at the same time that treatment mass index J_3 is minimized.

In Figure 5, it was shown that the optimization converges very quickly. Let us then analyze the variation of CL and SL total thicknesses, that is H_T and H_B, along generations. Figure 7 shows CL and SL thicknesses for initial population and for evolved populations, after 3 and 50 generations. Notice that within 3 generations, the parametric space is already reduced to a reasonably narrow optimal region. It reduces further then and, around the tenth generation, it collapses into the optimal solution, represented by the cross in Figure 7.

Figures 8 and 9 show the total thicknesses of CL and SL versus the viscoelastic layer thickness. It can be observed that the optimization converges very rapidly to a small viscoelastic layer thickness range (below 0.5 mm), although viscoelastic layer thicknesses of up to 3 mm were initially considered.

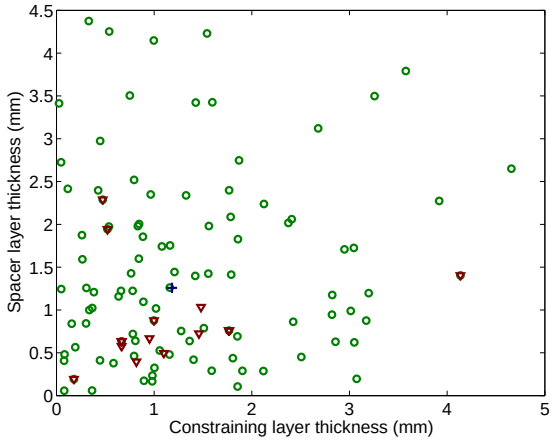

Figure 7: CL and SL total thicknesses for individuals of initial population (circles) and evolved populations, after 3 (triangle) and 50 (cross) generations.

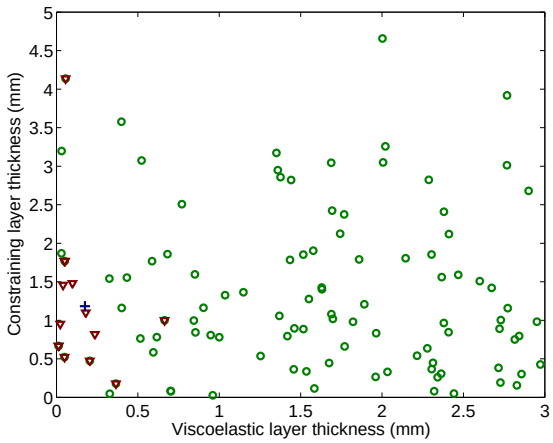

Figure 8: CL and viscoelastic layer thicknesses for individuals of initial population (circles) and evolved populations, after 3 (triangle) and 50 (cross) generations.

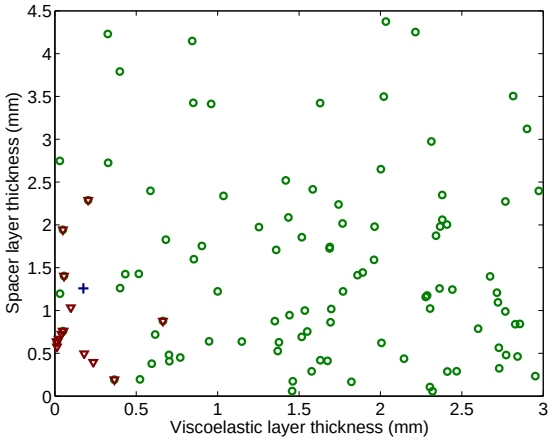

Figure 9: SL and viscoelastic layer thicknesses for individuals of initial population (circles) and evolved populations, after 3 (triangle) and 50 (cross) generations.

6 Conclusions

The geometrical optimization of passive damping treatments applied to laminated composite beams was presented. This is made using a finite element model able to handle sandwich beams with laminated surface layers and viscoelastic core. The frequency-dependence of the viscoelastic material properties was modeled using the Anelastic Displacement Fields model. A complex-based modal reduction was used and an equivalent real representation of the reduced-order system was constructed. The damping treatments consist of viscoelastic layers sandwiched between two composite layers. The upper one serving as constraining layer (CL) and the lower one as spacer (or stand-off) layer (SL). CL and SL plies number, thickness and orientation were considered as design parameters and were optimized using a genetic algorithm with eigenfrequency changes and weight constraints. A strategy for multicriteria optimization was presented using as performance indices the integral of transverse velocities, to be minimized, and the damping factors of the first five eigenmodes, to be maximized. In addition, the total mass of the treatment and the variation of the structure eigenfrequencies due to the treatment were used as penalty cost functions.

The results have shown that the use of a global cost function allows to optimize damping factors of the structure while minimizing the total mass of the damping treatment. However, it was found that less treatment mass may be obtained, with less damping also evidently, through modification of the weight parameters β_i. These should be valued according to design and operation conditions. The choice of GA for the optimization was shown to be adequate for the cases studied here, although for each generation the evaluation function must be calculated for each individual. Future works will be directed to the study of other multicriteria optimization techniques and the inclusion of decision rules to yield automatic updating of weight factors.

References

[1] R.L. Bagley and P.J. Torvik. Fractional calculus – a different approach to analysis of viscoelastically damped structures. *AIAA Journal*, 21(5):741–748, 1983.

[2] E. Balmès and A. Bobillot. Analysis and design tools for structures damped by viscoelastic materials. In *Proceedings of 20th International Modal Analysis Conference*, pages 210–216. SEM, 2002.

[3] D.A. Castello, F.A. Rochinha, N. Roitman, and C. Magluta. Modelling and identification of viscoelastic materials by means of a time domain technique. In J. Herskovits, S. Mazorche, and A. Canelas, editors, *6th World Congress of Structural and Multidisciplinary Optimization*, Rio de Janeiro, 2005. ISSMO.

[4] R.A. DiTaranto. Theory of vibratory bending for elastic and viscoelastic layered finite-length beams. *Journal of Applied Mechanics*, 32(4):881–886, 1965.

[5] J.J. Espíndola, J.M. Silva Neto, and E.M.O. Lopes. A generalised fractional derivative approach to viscoelastic material properties measurement. *Applied Mathematics and Computation*, 164(2):493–506, 2005.

[6] D. Goldberg. *Genetic algorithms in search, optimization, and machine learning.* Addison-Wesley Pub. Co., 1989.

[7] D.F. Golla and P.C. Hughes. Dynamics of viscoelastic structures – a time-domain, finite element formulation. *Journal of Applied Mechanics*, 52(4):897–906, 1985.

[8] M. Hao and M.D. Rao. Vibration and damping analysis of a sandwich beam containing a viscoelastic constraining layer. *Journal of Composite Materials*, 39(18):1621–1643, 2005.

[9] C.R. Houck, J. Joines, and M. Kay. A genetic algorithm for function optimization: A matlab implementation. Technical Report Technical Report NCSU-IE-TR-95-09, North Carolina State University, Raleigh, NC, 1995.

[10] E.M. Kerwin, Jr. Damping of flexural waves by a constrained visco-elastic layer. *Journal of the Acoustical Society of America*, 31(7):952–962, 1959.

[11] M.J. Lam, D.J. Inman, and W.R. Saunders. Variations of hybrid damping. In L.P. Davis, editor, *Smart Struct. & Mater. 1998: Passive Damping and Isolation*, volume 3327, pages 32–43, Bellingham (USA), 1998. SPIE.

[12] G.A. Lesieutre and E. Bianchini. Time domain modeling of linear viscoelasticity using anelastic displacement fields. *Journal of Vibration and Acoustics*, 117(4):424–430, 1995.

[13] G.A. Lesieutre and U. Lee. A finite element for beams having segmented active constrained layers with frequency-dependent viscoelastics. *Smart Materials and Structures*, 5(5):615–627, 1996.

[14] A.M.G. Lima, M.H. Stoppa, D.A. Rade, and V. Steffen Jr. Sensitivity analysis of viscoelastic structures. *Shock and Vibration*, 13(4-5):545–558, 2006.

[15] J.L. Marcelin, P. Trompette, and A. Smati. Optimal constrained layer damping with partial coverage. *Finite Elements in Analysis and Design*, 12(3-4):273–280, 1992.

[16] D.J. McTavish and P.C. Hughes. Modeling of linear viscoelastic space structures. *Journal of Vibration and Acoustics*, 115(1):103–110, 1993.

[17] D.J. Mead. *Passive Vibration Control*. John Wiley & Sons, New York, 1999.

[18] D.J. Mead and S. Markus. The forced vibration of a three-layer, damped sandwich beam with arbitrary boundary conditions. *Journal of Sound and Vibration*, 10(2):163–175, 1969.

[19] B.C. Nakra. Vibration control in machines and structures using viscoelastic damping. *Journal of Sound and Vibration*, 211(3):449–465, 1998.

[20] M.D. Rao. Recent applications of viscoelastic damping for noise control in automobiles and commercial airplanes. *Journal of Sound and Vibration*, 262(3):457–474, 2003.

[21] L.A. Silva, E.M. Austin, and D.J. Inman. Time-varying controller for temperature-dependent viscoelasticity. *Journal of Vibration and Acoustics*, 127(3):215–222, 2005.

[22] V. Steffen Jr., D.A. Rade, and D.J. Inman. Using passive techniques for vibration damping in mechanical systems. *Journal of the Brazilian Society of Mechanical Sciences*, 22(3):411–421, 2000.

[23] M.A. Trindade and A. Benjeddou. Hybrid active-passive damping treatments using viscoelastic and piezoelectric materials: review and assessment. *Journal of Vibration and Control*, 8(6):699–746, 2002.

[24] M.A. Trindade, A. Benjeddou, and R. Ohayon. Finite element analysis of frequency- and temperature-dependent hybrid active-passive vibration damping. *Revue Europenne des Élments Finis*, 9(1-3):89–111, 2000.

[25] M.A. Trindade, A. Benjeddou, and R. Ohayon. Modeling of frequency-dependent viscoelastic materials for active-passive vibration damping. *Journal of Vibration and Acoustics*, 122(2):169–174, 2000.

[26] M.A. Trindade, A. Benjeddou, and R. Ohayon. Finite element modeling of hybrid active-passive vibration damping of multilayer piezoelectric sandwich beams – part 1: Formulation. *International Journal for Numerical Methods in Engineering*, 51(7):835–854, 2001.

[27] M.A. Trindade, A. Benjeddou, and R. Ohayon. Piezoelectric active vibration control of sandwich damped beams. *Journal of Sound and Vibration*, 246(4):653–677, 2001.

[28] H. Zheng, C. Cai, and X.M. Tan. Optimization of partial constrained layer damping treatment for vibrational energy minimization of vibrating beams. *Computers and Structures*, 82(29-30):2493–2507, 2004.

Appendix A Material properties

A.1 AS4/3501-6 carbon-epoxy composite material

The mass density and constitutive matrix for the AS4/3501-6 composite material are

$$\rho_c = 1389.23 \text{ kg m}^{-3}$$

$$\mathbf{Q}(0) = \begin{bmatrix} 1.494 & 0.057 & 0.057 & 0 & 0 & 0 \\ 0.057 & 0.108 & 0.034 & 0 & 0 & 0 \\ 0.057 & 0.034 & 0.108 & 0 & 0 & 0 \\ 0 & 0 & 0 & 0.041 & 0 & 0 \\ 0 & 0 & 0 & 0 & 0.041 & 0 \\ 0 & 0 & 0 & 0 & 0 & 0.035 \end{bmatrix} 10^{11} \text{ N m}^{-2}$$

When rotating the composite ply of an angle ϕ around the z-axis leads to the following transformed constitutive matrix,

$$\mathbf{Q}(\phi) = \mathbf{T}\mathbf{Q}(0)\mathbf{T}^T$$

where

$$\mathbf{T} = \begin{bmatrix} (\cos\phi)^2 & (\sin\phi)^2 & 0 & -2\cos\phi\sin\phi & 0 & 0 \\ (\sin\phi)^2 & (\cos\phi)^2 & 0 & 2\cos\phi\sin\phi & 0 & 0 \\ 0 & 0 & 1 & 0 & 0 & 0 \\ \cos\phi\sin\phi & -\cos\phi\sin\phi & 0 & (\cos\phi)^2 - (\sin\phi)^2 & 0 & 0 \\ 0 & 0 & 0 & 0 & \cos\phi & -\sin\phi \\ 0 & 0 & 0 & 0 & \sin\phi & \cos\phi \end{bmatrix}$$

Then, after reduction of three-dimensional constitutive matrices due to the xy plane-stress assumption, modified elastic constants become

$$Q_{11}^* = Q_{11} - \frac{Q_{13}^2}{Q_{33}}$$

A.2 3M ISD112 viscoelastic material

The master curves for 3M ISD112 viscoelastic material at 27°C were given in Figure 2. The three ADF series of parameters used to curve-fit the material data are as following

$$G_0 = 0.50 \text{ MPa} \; ; \; \Delta = [0.7456, 3.2647, 43.2840]$$

$$\Omega_i = [468.69, 4742.36, 71532.49] \text{ rad/s}$$

Moreover, its Poisson's ratio equals approximately 0.49. Hence, the Young's modulus may be evaluated from $G^*(\omega)$ such that $E^*(\omega) = 2.98G^*(\omega)$. Its mass density is $\rho_v = 1000$ kg m^{-3}.